

Shrinking Core Model for the Discharge of a Metal Hydride Electrode

Venkat R. Subramanian,* Harry J. Ploehn, and Ralph E. White**

Center for Electrochemical Engineering, Department of Chemical Engineering, University of South Carolina, Columbia, South Carolina 29208, USA

A shrinking core model is presented for the galvanostatic discharge of a metal hydride particle. A quantitative criterion for when the shrinking core can be completely neglected or approximated by a pseudosteady-state solution is presented. The effect of shrinking of the core on the discharge behavior of a metal hydride particle is also studied.

© 2000 The Electrochemical Society. S0013-4651(00)01-086-7. All rights reserved.

Manuscript submitted January 24, 2000; revised manuscript received April 28, 2000.

Metal hydride particles are used to make negative electrodes¹⁻³ in nickel/metal hydride batteries. The performance of these electrodes is affected by both the kinetics of the processes occurring at the metal-electrolyte interface and the hydrogen diffusion within the bulk of the metal alloy particle. Two different phases exist in the metal hydride particles. The hydriding or charging process of metal hydride particles was discussed in detail in Ref. 4 where equations governing the diffusion of hydrogen in the particle during charging (hydriding) were derived from the fundamental laws of mass and momentum transfer. Zhang *et al.*⁴ were the first to develop rigorous boundary conditions based on jump balances. They provided a closed-form solution for the charging of metal hydride electrodes assuming a known (constant) concentration at the surface. They derived expressions describing the motions of the α - β interface and the weight fraction of hydrogen entering the electrode particle from the electrolyte. They predicted that for particles of smaller radius and smaller diffusion coefficients, the pseudosteady-state (PSS) solution⁵⁻¹² does not provide an accurate solution of the governing equations. Unfortunately, their model cannot be used to predict the effect of applied current density on the concentration profiles and charge/discharge curves for the metal hydride electrodes.

The discharge process of a metal hydride particle includes a phase change as shown schematically in Fig. 1. In the fully charged state (Fig. 1a) the metal hydride particle is in the β phase. The discharge process begins when the adsorbed hydrogen (H_{ads}) at the surface of the particle reacts electrochemically with hydroxide ions as follows



The consumption of the adsorbed hydrogen at the surface promotes the formation of the α phase (hydrogen-depleted metal hydride ma-

terial) as shown in Fig. 1b. Next, the adsorbed hydrogen that is consumed at the surface of the particle is replenished by diffusion of hydrogen atoms from the metal hydride β phase through the α phase to the surface. The discharge process is complete when the hydrogen from the metal hydride material has been consumed and the particle consists of the α phase only. The discharge process was modeled approximately by Lei and Wang *et al.*^{13,14}

In this paper shrinking of the β phase core is modeled assuming a constant applied current at the particle surface. This provides a means for one to predict the effect of applied current density on the concentration profiles and discharge curves. A closed-form time-dependent solution for the hydrogen concentration and the interface position is developed for the discharge process. Then, using the anodic polarization equation, surface potential is calculated. A quantitative criterion for when the shrinking β phase core can be completely neglected (*i.e.*, replaced by simple spherical diffusion) or approximated by a PSS solution is developed and presented.

Mathematical Model for the Discharge Process

The discharge of a spherical metal hydride particle is assumed to follow the sequence described previously (see Fig. 1). The assumed picture of the hydrogen concentration inside the particle electrode shortly after discharge begins is presented in Fig. 2a. The hydrogen within the metal hydride is initially at a concentration c_0 . Upon discharge, hydrogen is depleted from the surface of the particle where the concentration is c_s . The concentration at the interface between the α and β phases is c_α . As the particle is discharged, the core of fully hydrided material (β phase) shrinks, as shown in Fig. 2b. The concentration $c(r)$ in the α phase ($r_c \leq r \leq R_p$) decreases continuously from c_α (at the interface) to c_s at $r = R_p$, as shown in Fig. 2b. The concentration of the hydrogen in the β phase is assumed to remain constant at c_0 .

The concentration distribution of the hydrogen atoms in the α phase is governed by

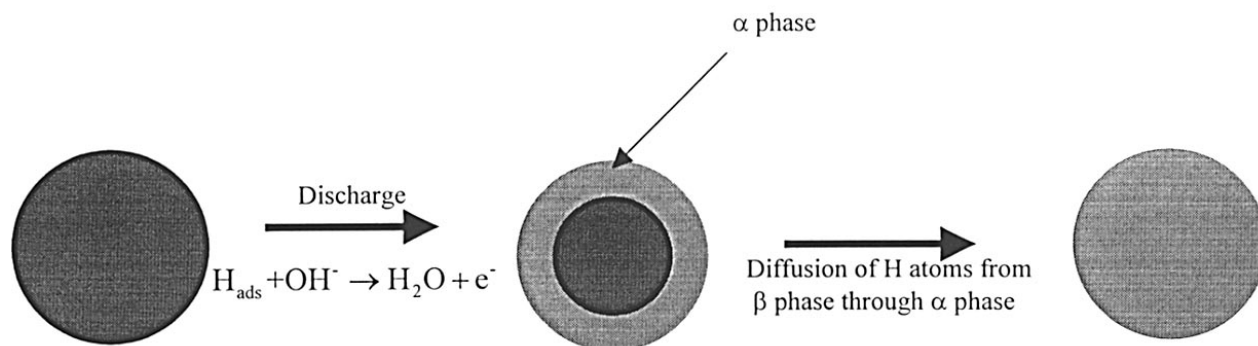


Figure 1. Schematic representation of the shrinking core during the discharge of a metal hydride particle: (a, left) β phase (completely charged state), (b, middle) $\alpha + \beta$ phase, and (c, right) α phase (completely discharged state).

* Electrochemical Society Student Member.

** Electrochemical Society Fellow.

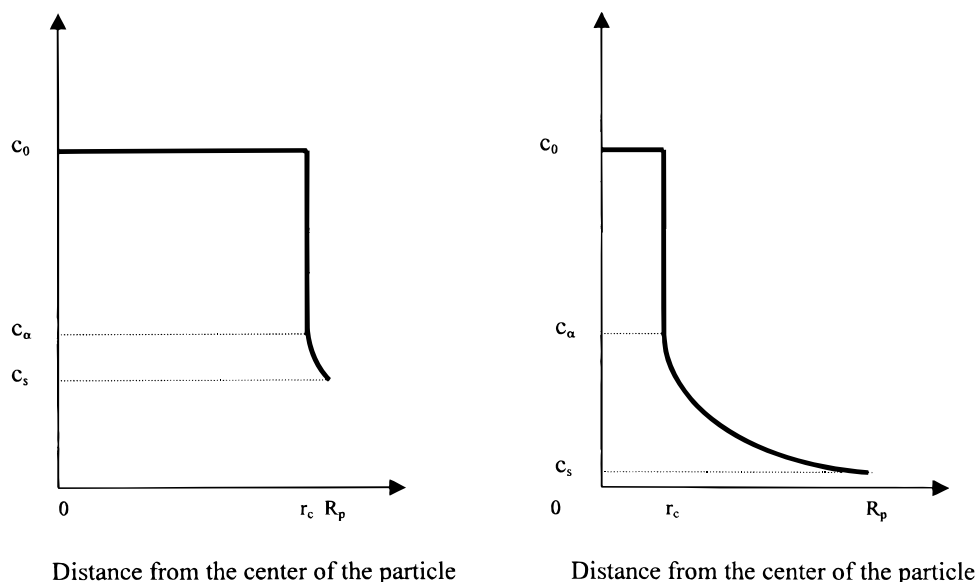


Figure 2. Concentration profiles inside in a spherical metal hydride electrode: (a, far left) shortly after discharge begins and (b, left) near the end of discharge.

$$\frac{\partial c}{\partial t} = \frac{D_\alpha}{r^2} \frac{\partial}{\partial r} \left(r^2 \frac{\partial c}{\partial r} \right) \quad [2]$$

where we have assumed that the diffusion coefficient for hydrogen atoms in the α phase, D_α , is a constant. The initial condition is known (completely charged, Fig. 1a). That is

$$c = c_0 \quad t = 0, 0 \leq r \leq R_p \quad [3]$$

The surface boundary condition is given by the current density applied at the surface

$$D_\alpha \frac{\partial c}{\partial r} = -\frac{i}{F} \quad t > 0, r = R_p \quad [4]$$

where i is the applied current density at the surface. The concentration at the moving interface (α/β interface) is assumed to be a known constant¹³ (Fig. 2)

$$c = c_\alpha \quad t > 0, r = r_c \quad [5]$$

where r_c , the shrinking core interface position, depends on time. The motion of the interface is governed by the mass flux at the interface¹³

$$(c_0 - c_\alpha) \frac{dr_c}{dt} = D_\alpha \frac{\partial c}{\partial r} \Big|_{r=r_c} \quad [6]$$

with the initial condition $r_c = R_p$ at $t = 0$, and c_0, c_α are known constants. The following dimensionless variables are introduced for convenience

$$\tau = \frac{D_\alpha t}{R_p^2} \quad x_c = \frac{r_c}{R_p} \quad x = \frac{r}{R_p} \quad C = \frac{c}{c_\alpha} \quad [7]$$

Substituting these dimensionless variables into Eq. 2 yields

$$\frac{\partial C}{\partial \tau} = \frac{1}{x^2} \frac{\partial}{\partial x} \left(x^2 \frac{\partial C}{\partial x} \right) \quad [8]$$

and the initial and boundary conditions become

$$\text{at } \tau = 0 \quad \text{for } 0 \leq x \leq 1 \quad C = C_0 \quad [9]$$

$$\text{for } \tau > 0, x = 1 \quad \frac{\partial C}{\partial x} = -\delta \quad [10]$$

$$\text{for } \tau > 0, x = x_c \quad C = 1 \quad [11]$$

where C_0 is the dimensionless initial concentration, and δ is the dimensionless current density, which can be thought of as the reaction rate relative to the diffusion rate and is given by

$$\delta = \frac{iR}{FD_\alpha c_\alpha} \quad [12]$$

The interface position is given by

$$\frac{dx_c}{d\tau} = k \frac{\partial C}{\partial x} \Big|_{x=x_c} \quad [13]$$

where

$$k = \frac{1}{C_0 - 1} \quad [14]$$

with the initial value of $x_c = 1$ at $\tau = 0$. The dimensionless concentration profile C in the α phase depends on the interface position x_c and hence depends on the parameter k . The applied current density in Eq. 12 can be expressed in terms of applied current per gram of the particle

$$i = \frac{\text{current}}{\text{area}} = \frac{\text{current}}{\text{mass}} \frac{\text{mass}}{\text{volume}} \frac{\text{volume}}{\text{area}} = I\rho \frac{\frac{4}{3}\pi R_p^3}{4\pi R_p^2} = \frac{I\rho R_p}{3} \quad [15]$$

where ρ is the density of the particle and I is the applied current per gram of the particle. Equation 15 can be used to modify Eq. 12

$$\delta = \frac{iR_p}{FD_\alpha c_\alpha} = \frac{I\rho R_p^2}{3FD_\alpha c_\alpha} \quad [16]$$

The boundary condition at $x = 1$ is not homogeneous and suggests a transformation of the form¹⁵

$$C = u(x, \tau) + w(x) \quad [17]$$

This transformation simplifies the problem to

$$\frac{1}{x^2} \frac{d}{dx} \left(x^2 \frac{dw}{dx} \right) = 0 \quad [18]$$

with the boundary conditions

$$\text{at } x = x_c \quad w = 1 \tag{19}$$

$$\text{at } x = 1 \quad \frac{dw}{dx} = -\delta \tag{20}$$

Using these boundary conditions w can be solved to give

$$w = 1 + \delta \left(\frac{1}{x} - \frac{1}{x_c} \right) \tag{21}$$

and

$$\frac{\partial u}{\partial \tau} = \frac{1}{x^2} \frac{\partial}{\partial x} \left(x^2 \frac{\partial u}{\partial x} \right) \tag{22}$$

with the initial and boundary conditions

$$\text{at } \tau = 0 \text{ for } 0 \leq 1 \quad u = C_0 - \left[1 + \delta \left(\frac{1}{x} - \frac{1}{x_c} \right) \right] \tag{23}$$

$$\text{or } \tau > 0, \quad x = 1 \quad \frac{\partial u}{\partial x} = 0 \tag{24}$$

$$\text{for } \tau > 0, \quad x = x_c \quad u = 0 \tag{25}$$

Now u can be solved with these homogeneous boundary conditions by separation of variables¹⁵ to give

$$u(x, \tau) = \frac{1}{x} \sum_{n=1}^{\infty} B_n \sin[\lambda_n(x - x_c)] \exp(-\lambda_n^2 \tau) \tag{26}$$

where the eigenvalue λ_n is given by

$$\tan[\lambda_n(1 - x_c)] = \lambda_n \quad n = 1, 2, \dots, \infty \tag{27}$$

The constant B_n can be found by using the initial condition and the procedure demonstrated in Ref. 15. After applying the initial condition and transforming back to dimensionless concentration C

$$C = 1 + \delta \left[\frac{1}{x} - \frac{1}{x_c} \right] - \frac{2}{x} \left[\sum_{n=1}^{\infty} A_n \sin[\lambda_n(x - x_c)] \exp(-\lambda_n^2 \tau) \right] \tag{28}$$

where

$$A_n = \frac{x_c(C_0 - 1) + \delta \cos[\lambda_n(1 - x_c)]}{\lambda_n(x_c - \sin^2[\lambda_n(1 - x_c)])} \tag{29}$$

and x_c is obtained by integrating Eq. 13 as explained in the following.

Solution Procedure

Equation 28 is an analytical solution that depends on x_c , which also depends on time. Consequently, to obtain $C(x, \tau)$ for given parameter values ($c_0, c_\alpha, I, k, \rho, R_p$, and D_α , see Table I), the first step is to set x_c equal to a value (0.99, e.g.) and solve Eq. 27 for the first five (say) eigenvalues ($\lambda_n, n = 1, 5$). Next, decrement x_c (0.98, e.g.) and solve again for the first five eigenvalues from Eq. 27. This procedure was repeated for x_c down to 0. The value for the first five eigenvalues obtained in this manner are presented in Fig. 3. These results are replotted in Fig. 4 to show that the eigenvalues are linearly related to $1/(1 - x_c)$.

Next, Eq. 13 is integrated numerically by explicit stepping. This process can be carried out by specifying a value for $\Delta\tau$ and using the following equation

$$x_c(\tau + \Delta\tau) = x_c(\tau) + \Delta\tau \left(k \frac{\partial C}{\partial x} \Big|_{x=x_c} \right) \tag{30}$$

Table I. Parameters used.

Parameters	Values	Reference
c_0	$91.3 \times 10^{-3} \text{ mol/cm}^3$	16
c_α	$10.7 \times 10^{-3} \text{ mol/cm}^3$	Assumed
D^α	$0.1 \times 10^{-10} \text{ mol}$	16
Q	310 mAh/g	16
I_0	14.24 mA/g	16
k (from Eq. 14)	0.1316	13
R_p	5 μm	16
T	298 K	Assumed
α	0.5	16
ϕ_0	-0.923 V (vs. Hg/HgO)	16
C_{rate}	310 mA/g ($\delta = 19.52$)	16
ρ	7.8 g/cm ³	Assumed

where $x_c(\tau = 0) = 1$ and the gradient in Eq. 30 is obtained from Eq. 28. This process can be continued until the dimensionless surface concentration becomes zero.

Pseudosteady-State Solution (PSS)

A PSS is obtained by assuming that at a particular time, for a particular value of the shrinking core radius, x_c , the concentration profiles

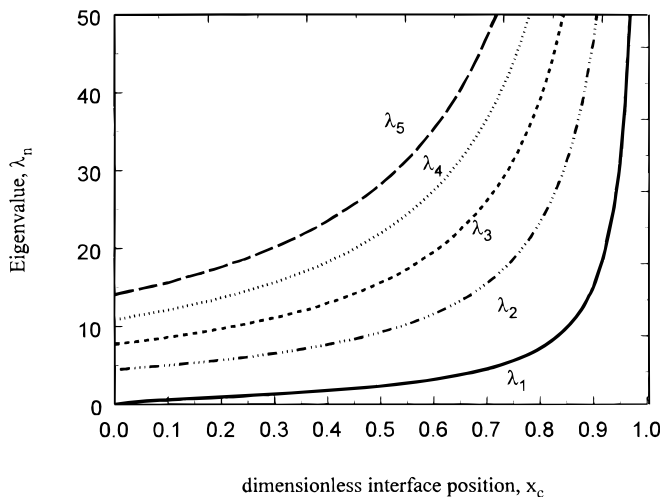


Figure 3. A plot of the first five eigenvalues as a function of dimensionless interface position.

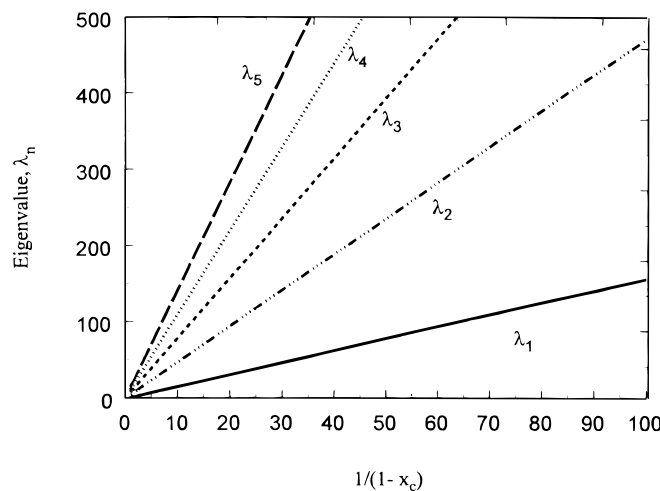


Figure 4. A plot of first five eigenvalues as a function of $1/(1 - x_c)$.

inside the particle are at steady state. This solution is obtained by equating the left side of Eq. 8 to zero which yields (see Eq. 21)

$$C_{\text{PSS}} = w = 1 + \delta \left(\frac{1}{x} - \frac{1}{x_c} \right) \quad [31]$$

Substituting this solution into Eq. 13 followed by integration yields

$$x_c = (1 - 3k\delta\tau)^{\frac{1}{3}} \quad [32]$$

which is plotted in Fig. 5 for comparison to the complete model. The PSS solution for the dimensionless concentration can be explicitly written in terms of dimensionless time as follows

$$C_{\text{PSS}} = 1 + \delta \left(\frac{1}{x} - \frac{1}{(1 - 3k\delta\tau)^{\frac{1}{3}}} \right) \quad [33]$$

Also, by substituting the right side of Eq. 16 into Eq. 33 we get the dimensional form

$$c_{\text{PSS}} = c_{\alpha} + \frac{I\rho R_p^2}{3D_{\alpha}F} \left(\frac{R_p}{r} - \frac{R_p}{r_c} \right) \quad [34]$$

and the surface concentration is given by substituting $r = R_p$ into Eq. 34

$$C_{\text{PSS}}(r = R_p) = c_{\alpha} - \frac{I\rho R_p^2}{3D_{\alpha}F} \left(\frac{R_p}{r} - 1 \right) \quad [35]$$

Equation 35 is the same as that presented by Lei *et al.*¹³ This PSS solution (Eq. 35) is compared to the exact transient solution and its validity is discussed in the following section. The dimensionless time for complete discharge according to this PSS model can be found by equating the surface concentration ($x = 1$ in Eq. 33) to zero

$$\tau_{\text{disch(PSS)}} = \frac{1 + 3\delta + 3\delta^2}{3k\delta(1 + 3\delta + 3\delta^2 + 3\delta^3)} \quad [36]$$

Discharge Curves

The kinetics at the surface of the particle can be written as an anodic process¹³

$$I = I_0 C_s \exp\left(\frac{\alpha F \eta}{RT}\right) \quad [37]$$

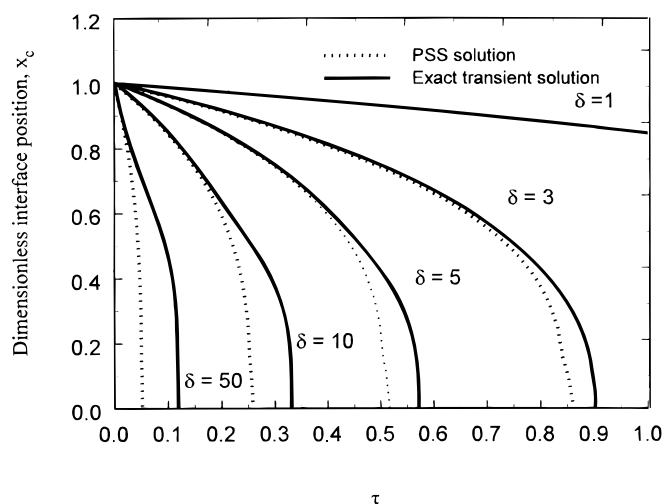


Figure 5. Dimensionless interface position as a function of dimensionless time for various values of δ during discharge ($k = 0.316$).

where C_s is the dimensionless surface concentration and I_0 is the exchange current per unit mass. The potential at the surface is given by¹⁶

$$E(\text{V}) (\text{vs. Hg/HgO}) = \phi_0 + \eta \quad [38]$$

Equations 37 and 38 are used to predict the discharge curves. The procedure consists of first setting I and the parameter values c_0 , c_{α} , k , ρ , R_p , and D_{α} followed by solving the governing equations to obtain Eq. 28, which can be solved for $C_s(\tau)$ by setting $x = 1$. Next, once values have been set for I_0 , ϕ_0 , α , and τ , Eq. 37 can be used to solve for $\eta(\tau)$, which upon substitution into Eq. 38 yields $E(\tau)$. For an applied current (I A/g), the surface concentration, $C_s(\tau)$, is found from Eq. 28 and substituted into Eq. 37. For a particular time τ and C_s , η is solved using Maple's fsolve command. Once the overpotential η is found, Eq. 38 is used to find the potential. This procedure is repeated until a cutoff potential of $E = -0.5$ V is reached.

Results and Discussion

Figure 3 shows at the beginning of the discharge, when x_c is almost 1, all the eigenvalues are very big and the exact transient solution given by Eq. 28 reduces to the PSS solution (Eq. 30). This is true because the eigenvalues are large and consequently, the summation terms in the series in Eq. 28 become negligible.

Figure 5 presents both the exact transient solution developed here and the PSS solution given by Eq. 31. As can be seen in Fig. 5, the PSS solution underpredicts the time for the core to shrink for $\delta \geq 1$, but for low values of the parameter ($\delta \leq 0.5$), both PSS and transient solution coincide.

A plot of the dimensionless concentration profile inside the shrinking core particle is presented in Fig. 6. For an applied current ($\delta = 1$), at very low times, the concentration near the surface of the particle is close to C_{α} . As time increases, the surface concentration depletes very fast and the core shrinks. The concentration inside the core (*i.e.*, inside the β phase) remains constant at C_0 (see Fig. 2).

A plot of the dimensionless surface concentration is presented in Fig. 7. As expected, the surface concentration is depleted faster for higher discharge rates (δ). Also, we observe that the discharge time, which is the time taken for surface concentration to reach approximately zero, is highly dependent on the dimensionless current density, δ . Another approximate solution to the problem can be obtained by ignoring the shrinking core β phase followed by solving the diffusion equation (Eq. 2), with the same initial and boundary condition (Eq. 3 and 4) and Eq. 5 is replaced by symmetry boundary condition (flux = 0 at the center of the particle). The solution for this problem can be conveniently obtained by separation of variables.¹⁵ The error in discharge time can be written as

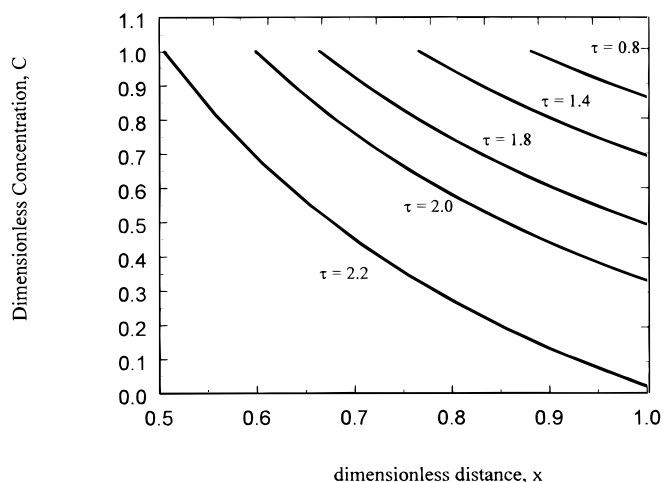


Figure 6. Dimensionless concentration profiles in the α phase at various times for $\delta = 1$.

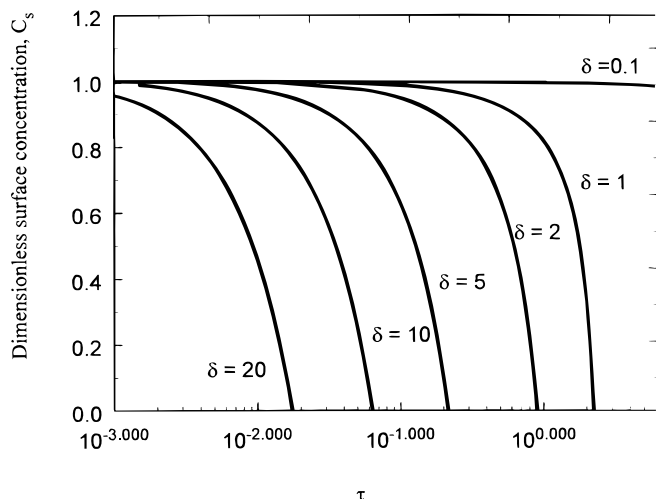


Figure 7. Surface concentration (dimensionless) as a function of dimensionless time for various values of δ .

$$\left. \begin{array}{l} \text{error (\%)} \\ \text{[sphere (no shrinking core)]} \end{array} \right\} = \frac{\text{abs}(\tau_{\text{disch(exact)}} - \tau_{\text{disch(sph)}})}{\tau_{\text{disch(exact)}}} \times 100 \quad [39]$$

Similarly the error in PSS model can be represented as

$$\left. \begin{array}{l} \text{error (\%)} \\ \text{(in PSS approximation)} \end{array} \right\} = \frac{\text{abs}(\tau_{\text{disch(exact)}} - \tau_{\text{disch(PSS)}})}{\tau_{\text{disch(exact)}}} \times 100 \quad [40]$$

Note that errors are predicted for both approximate models for $\delta > 1$ (Fig. 8). The error in approximating the shrinking core with the PSS solution is less than 10% for $\delta < 5$ (i.e., rates less than $C/4$ for $R_p = 5 \mu\text{m}$ particle). However for $\delta > 5$, the error shoots up and we observe more than 10% error. For 2C discharge ($\delta = 40$) the error in approximating the shrinking core with a PSS solution shoots up to 50% error.

Figure 8 illustrates clearly that the shrinking core cannot be neglected at high values of δ , which could be due to high values of ap-

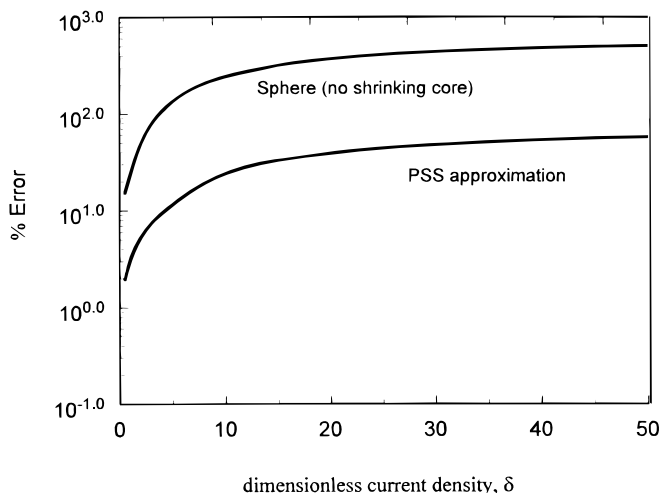


Figure 8. Error in neglecting or approximating shrinking core model.

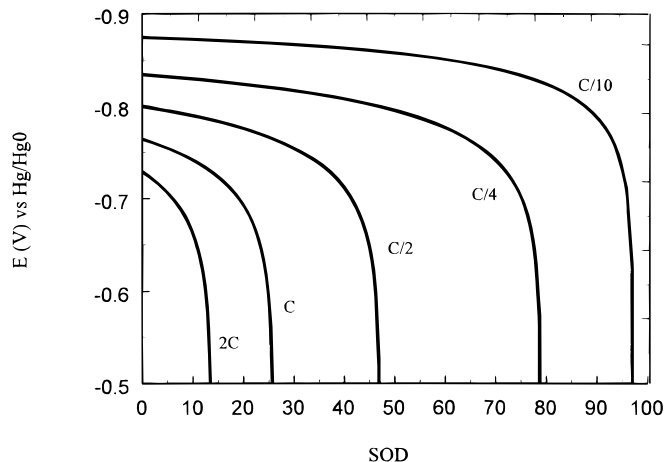


Figure 9. Effect of discharge rates on the surface potential: discharge curves on a shrinking electrode.

plied current (I), large values of R_p , or small values of D_α . This analysis also shows that the PSS solution could be used cautiously for small values of δ . For discharge rates less than $C/4$, PSS could be used with a 10% error. For discharge rates higher than $C/4$, the PSS solution should not be used. Note that the predictions depend on k , which has not been varied in this paper.

Discharge curves for different discharge rates are plotted in Fig. 9. The state of discharge (SOD) is defined here as

$$\text{SOD} = \frac{I(\text{current applied, A/g}) \times t(\text{second}) \times 100}{Q(\text{capacity, Ah/g}) \times 3600} \quad [41]$$

As expected, for higher discharge rates the particle discharges faster (E reaches -0.5 V in less time). Also, we observe that for very low rates (rates less than $C/10$), the predicted SOD of the electrode is approximately the same as that for a spherical particle (Fig. 10). However, with increasing discharge rates, the SOD of the particle at ($E = -0.5 \text{ V}$) with a shrinking core is much less than that predicted by the spherical particle model (Fig. 10), because hydrogen remains in the β phase and does not react at high discharge rates. Thus, for predicting the utilization accurately, especially at high discharge rates, the shrinking core model should be used. Also, at high discharge rates ohmic losses dominate and should be added for more accurate predictions.

Conclusions

A shrinking core model for the discharge of a metal hydride particle is presented. A PSS model is also presented. The predicted re-

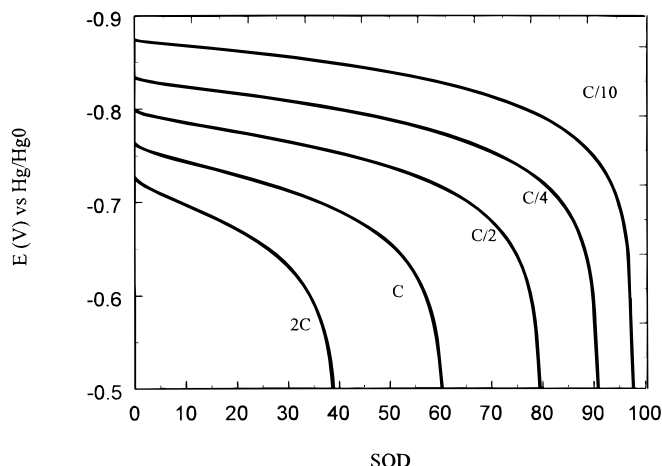


Figure 10. Discharge curves in a spherical electrode.

sults from the models show that the PSS approximation can be used cautiously for rates less than $C/4$ (for a $5\ \mu\text{m}$ particle). However, for discharge rates higher than $C/4$, the PSS model should not be used.

Acknowledgments

The authors are grateful for financial support of the project by the National Reconnaissance Organization (NRO) under contract no. 1999 I016400 000 000.

The University of South Carolina assisted in meeting the publication costs of this article.

List of Symbols

A_n	coefficient in the solution
B_n	coefficient in the solution
c	concentration, mol/cm ³
c_0	initial concentration (completely charged state), mol/cm ³
c_s	surface concentration, mol/cm ³
c_α	concentration at the α/β interface, mol/cm ³
C	dimensionless concentration, c/c_α
C_{rate}	rate of discharge, $I = 310\ \text{mA/g}$
C_{PSS}	dimensionless pseudosteady-state concentration
C_0	dimensionless initial concentration, c_0/c_α
C_s	dimensionless surface concentration, c_s/c_α
D_α	diffusion coefficient in the α phase, cm ² /s
e	electron
E	applied potential (V vs. Hg/HgO)
i	applied current density, A/cm ²
I	applied current, A/g
I_0	exchange current, A/g
k	dimensionless constant, $1/C_0 - 1$
n	index
r	radial position, cm
r_c	radial position of the α/β interface, cm
R	gas constant, 8.314 J/mol/K
R_p	metal alloy particle radius, cm
t	time, s
u	dependent variable
w	dependent variable

x	number of reactant atoms per unit of product; fractional conversion
x_c	dimensionless interface position, r_c/R_p

Greek

α	solid metal phase
α	transfer coefficient, 0.5
β	unreacted metal hydride phase
δ	dimensionless current density
λ	eigenvalue
ρ	mass density of particle, g/cm ³
τ	dimensionless time
τ_{disch}	discharge time, dimensionless
η	overpotential, V vs. Hg/HgO

Subscripts and superscripts

ads	adsorbed
H	hydrogen

References

1. G. Sandrock, in *Hydrogen and Metal Hydride Batteries*, P. D. Bennett and T. Sakai, Editors, PV 94-27, p. 219, The Electrochemical Society Proceedings Series, Pennington, NJ (1994).
2. T. H. Fuller and J. Newman, in *Modern Aspects of Electrochemistry*, R. E. White, J. O'M. Bockris, and B. E. Conway, Editors, Vol. 27, p. 359, Plenum Press, New York (1993).
3. H. F. Bittner and C. C. Badcock, *J. Electrochem. Soc.*, **130**, 193C (1983).
4. W. Zhang, S. Srinivasan, and H. J. Ploehn, *J. Electrochem. Soc.*, **143**, 4039 (1996).
5. S. Yagi and D. Kunii, *Chem. Eng. Sci.*, **16**, 364 (1961).
6. K. B. Bischoff, *Chem. Eng. Sci.*, **18**, 711 (1963).
7. J. R. Bowen, *Chem. Eng. Sci.*, **20**, 712 (1965).
8. K. B. Bischoff, *Chem. Eng. Sci.*, **20**, 783 (1965).
9. T. G. Theofanous and H. C. Lim, *Chem. Eng. Sci.*, **25**, 1927 (1970).
10. N. Lindman and D. Simonsson, *Chem. Eng. Sci.*, **34**, 31 (1979).
11. G. F. Carey and P. Murray, *Chem. Eng. Sci.*, **44**, 979 (1989).
12. P. Carabin and D. Berk, *Chem. Eng. Sci.*, **47**, 2499 (1992).
13. Y. Q. Lei, C. S. Wang, X. G. Yang, H. G. Pan, J. Wu, and Q. D. Wang, *J. Alloys Compd.*, **231**, 611 (1995).
14. C. S. Wang, Y. Q. Lei, and Q. D. Wang, *Electrochim. Acta*, **43**, 3193 (1998).
15. V. R. Subramanian and R. E. White, in *Tutorials in Electrochemical Engineering-Mathematical Modeling*, R. E. Savinell, J. M. Fenton, A. C. West, S. L. Scanlon, and J. Weidner, Editors, PV 99-14, p. 100, The Electrochemical Society Proceedings Series, Pennington, NJ (1999).
16. B. S. Haran, B. N. Popov, and R. E. White, *J. Electrochem. Soc.*, **145**, 3000 (1998).